ACS OMEGA

http://pubs.acs.org/journal/acsodf

Article

Synthesis of Biomass-Derived Activated Carbons and Their Immobilization on Alginate Gels for the Simultaneous Removal of Cr(VI), Cd(II), Pb(II), As(III), and Hg(II) from Water

Aditya Kumar, Triparna Das, Ravindra Singh Thakur, Zeenat Fatima, Satgur Prasad, Nasreen G. Ansari,*,§ and Devendra K. Patel*,§

Cite This: *ACS Omega* 2022, 7, 41997−42011

Read Online

ACCESS | Metrics & More | Article Recommendations | Supporting Information

ABSTRACT: Low-cost alginate gels of activated carbons were prepared, which were derived from the peels of banana and sweet lime. The synthesized carbon was activated and immobilized on alginate, producing its gel. These gels were categorized according to their methods of drying, in which air drying, freeze drying, and supercritical drying led to the formation of xerogels, cryogels, and aerogels, respectively. The gels were used for adsorption of heavy metals from their aqueous solution. The heavy metals that were targeted for removal were Pb(II), Cd(II), Cr(VI), As(III), and Hg(II). Among all the adsorbents, the alginate cryogel of sweet lime-derived activated carbon (SLACC) showed the highest removal percentage of heavy metals, and thus, it was used for batch study. The adsorption of heavy metals by SLACC was checked at different times, pH values, adsorbent doses, temperatures, and adsorbate concentrations. The study revealed that the pseudo-second-order model best described the kinetic study, while the adsorption followed the Freundlich isotherm. SLACC showed maximum adsorption capacities (q_{cal}) of 3.71, 4.22, 20.04, 7.31, and 4.37 mg/g for Cr, Cd, Pb, As, and Hg, respectively, when 20 mg of SLACC was used for the removal of 4 ppm concentration of the targeted heavy metals from their 20 mL solution. Based on the thermodynamic study, it was found that the adsorption was spontaneous and exothermic. Furthermore, the adsorbent was also used on real water samples and showed up to 90% removal efficiency for these targeted heavy metals. SLACC was regenerated with 0.1 M ethylenediaminetetraacetic acid (EDTA) solution and reused for five cycles, in which the percentage removal of heavy metals was more than 50% till the fourth cycle. Furthermore, the leaching study showed that no toxic elements had leached from SLACC into water, making it a safe adsorbent.

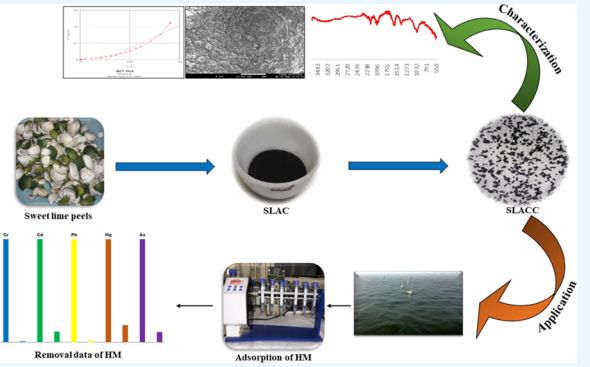

1. INTRODUCTION

The periodic elements having a high density (3−7 g/cm^3) and atomic number are generally regarded as heavy metals (HMs).[1] Among all naturally occurring elements, 53 elements are considered HMs, in which most of them belong to the transition elements, while lanthanides, actinides, and some p-block elements (like As) also come under this category.[2] In the environment, HMs can be produced both naturally and anthropogenically. Naturally, they are introduced into the environment by forest fires, volcanic eruptions, and leaching of rocks, but most of their environmental presence is due to human activities, mainly by industrialization (smelting, mining, metal plating).[3] Unlike many organic contaminants, HM are non-biodegradable or persistent, making them more dangerous for living beings.[4] There are some HMs including Zn, Mn, Cu, etc. that act as a micronutrient for the humans but are toxic if consumed in higher amounts.[5] Thus, HMs are required to be monitored, and in this regard, various steps have been taken to reduce their levels below the permissible limits.[6] Heavy metals such as Pb(II), Cr(VI), Cd(II), As(III), and Hg(II) are highly toxic to living organisms even if present in trace amounts and are listed in the USEPA list of priority pollutants.[7] They can cause nervous system disorder, gastrointestinal problems, and cardiovascular collapse in humans.[8]

Water is one of the most important components for survival of living organisms. It is well known that the availability of drinking water is a global concern, and with the rapid increase of industrialization, the quality of water is deteriorating day by day.[9] HMs quickly find ways to enter into the water bodies by dumping of industrial or household wastes or through leaching from sludge, thereby increasing the levels of HMs in water. Consumption of any of the toxic HMs (which are present

Received: June 17, 2022
Accepted: October 27, 2022
Published: November 8, 2022

above their permissible limit) either directly or indirectly could be lethal for life.[10] Therefore, due to the high toxicity of HMs, it is essential to come up with the idea or technology that can decontaminate HMs from water and make it safe for human consumption.[11] There are many existing techniques that are available for the removal of contaminants from water such as ion exchange, electrokinetic membranes, chemical precipitation, electrocoagulation, membrane filtration, and microbial remediation.[3,12] These technologies have various shortcomings such as high cost, generation of toxic waste, disposal issue, and high power consumption.[5] Therefore, there is a need of developing a technology or material that is cheap, effective, and eco-friendly for the removal of HMs. In recent years, the adsorption process (particularly biosorption) has been proved to be effective. Many researchers worldwide have developed different adsorbents for the elimination of HMs.[13] Several researchers have used activated carbon (AC), biochar, and biochar-derived activated carbon for the removal of HMs, which proved to be highly effective because of their high surface area.[14] Biochar derived from sugarcane bagasse and orange peel had shown efficiency in the removal of Pb(II) from aqueous solution, while apricot-derived activated carbon showed efficiency for the removal of Ni(II), Cd(II), Co(II), Pb(II), Cu(II), Cr(VI), and Cr(III) from aqueous solution because of the high surface area and presence of functional groups on their surface.[15,16] Despite the effectiveness, their removal (recovery from solution after adsorption) and dumping (or disposal) are still an issue. This issue can be overcome by immobilizing activated carbon on materials or gels that can be easily removed and reused. At the same time, they should be nontoxic, cheap, and good enough for adsorption of HMs.[17] Alginate gels or alginate beads have proved to be highly useful for adsorption of HMs and showed even better results after immobilization with activated carbon.[18]

Alginate is a natural polysaccharide that forms the structural component of the algal cell wall. It is formed by copolymerization of α-L-guluronic acids (G-block) and β-D-mannuronic acids (M-block), held together by 1−4 linkage.[19] It contains −COOH and −OH groups, due to which it acts as a metal chelator. In the past few years, alginate has been widely used for elimination of organic and inorganic contaminants from water. It acts as an excellent support material and shows enhanced activity when immobilized with appropriate compounds.[17] Alginate has a property of forming water-insoluble irreversible gels when it comes in contact with polyvalent cations including Ca^{2+} ($CaCl_2$) and Fe^{3+} (from $FeCl_3$). This forms a system of cage-like structure of cation−alginate gels.[20] The resulting gels can be further categorized according to their methods opted for drying, in which drying of gels at room temperature results in xerogel formation, while freeze drying of gels and drying gels at supercritical temperature result in the formation of cryogels and aerogels, respectively.[21−23] These gels not only show good adsorption capacities but also are cheap and environment-friendly.[24,25]

In this study, two types of biochar were prepared from the peels of sweet lime and banana since these two fruits are widely consumed in India and generate good amounts of peels. To increase the efficiency of these two biochars, both of them were converted into their respective activated carbons with the help of KOH that acts as an activating agent.[26] Furthermore, these two activated carbons and commercial activated carbon were immobilized on alginate separately, producing xerogel, cryogel, and aerogel of each of the three activated carbons. Three blank gels (cryogel, aerogel, and xerogel without activated carbon) of alginate were also prepared for comparative studies. Application of these gels was checked for the removal of As(III), Hg(II), Cr(VI), Cd(II), and Pb(II) from their aqueous solution. Their performance was investigated at varying temperatures, contact times, adsorbent doses, pH values, and initial concentrations of the adsorbate. Furthermore, their adsorption and kinetic modeling have also been characterized to understand the mechanism of adsorption.

2. MATERIALS AND METHODS

2.1. Materials. Lead nitrate ($Pb(NO_3)_2$), cadmium chloride ($CdCl_2$), potassium dichromate ($K_2Cr_2O_7$), sodium arsenite ($NaAsO_2$), mercuric chloride ($HgCl_2$), activated carbon, calcium chloride ($CaCl_2$), and sodium alginate were purchased from Sigma-Aldrich. Analytical-grade potassium hydroxide (KOH), sodium hydroxide (NaOH), ethylenediaminetetraacetic acid (EDTA), conc. HNO_3, and conc. HCl were purchased from Merck, Germany. Ultrapure water (Milli-Q) was obtained from CSIR-IITR, India. Reference standards of heavy metals (1000 mg/mL) of high purity traceable to the NIST standard reference material (SRM) were purchased from Merck, Darmstadt, Germany. For the adsorption experiment, 1000 ppm (or mg/L) mixed solution of Pb(II), Cd(II), Cr(VI), As(III), and Hg(II) was prepared from salts of $Pb(NO_3)_2$, $CdCl_2$, $K_2Cr_2O_7$, $NaAsO_2$, and $HgCl_2$, respectively in Milli-Q water and diluted using 1% HNO_3 to 4 ppm. For the quantitative analysis, a working standard of 100 ppm was prepared from the 1000 ppm mixed standard of heavy metals. From this working standard, solutions of concentrations of 1, 2, 3, 5, and 10 ppm were prepared to obtain a calibration graph.

2.2. Preparation of Activated Carbons Derived from the Peels of Sweet Lime and Banana. Peels of sweet lime and banana were collected from a local fruit shop in Lucknow, India. They were cut into small bits and repeatedly washed with tap water to remove dust particles and impurities. Then, both peels were air-dried for 7 days and then dried in an oven at 90 °C for 36 h. The dried peels were ground to powder and then sieved. The powdered peels were carbonized at a temperature of 650 °C for 3 h using a muffle furnace and then cooled at room temperature. The resulting biochar was activated with KOH for which biochar and KOH were mixed in a ratio of 1:3 using ultrapure water and left overnight. This mixture was then dried at 120 °C in an oven followed by its activation at 700 °C for 4 h using a muffle furnace. After that, the product was cooled at room temperature and then washed with distilled water repeatedly to remove any residual impurities. The final product was dried at 80 °C for 1 h to get activated carbon.[16] The activated carbon derived from the peels of sweet lime was named as SLAC, while that from banana peels was named as BAC. For comparison of these activated carbons, commercial activated carbon (AC) was also used in this study.

2.3. Preparation of Activated Carbon (SLAC, BAC, and AC)-Immobilized Alginate Gels. The gels were prepared by an ionic gelation method in which SLAC was immobilized into the alginate gel by dissolving 5 g of sodium alginate and 5 g of SLAC in 500 mL of Milli-Q, using a magnetic stirrer. This mixture was dropped into $CaCl_2$ solution (0.5 M), by means of a peristaltic pump to form uniform spherical-shaped beads or

https://doi.org/10.1021/acsomega.2c03786
ACS Omega 2022, 7, 41997−42011

gel due to the crosslinking of alginate molecules by Ca^{2+}.[18] These semisolid beads were left overnight in the same solution for proper crosslinking and hardening of beads. The beads were divided into three parts, in which one part was air-dried to get the alginate xerogel of SLAC (SLACX), the second part was freeze-dried to get the alginate cryogel of SLAC (SLACC), and the third part was supercritical-dried to get the alginate aerogel of SLAC (SLACA).[18] Similarly, BAC-immobilized gels were also prepared by this method and named as BAC alginate xerogel (BACX), BAC alginate cryogel (BACC), and BAC alginate aerogel (BACA). For comparison, three gels (aerogel, cryogel, and xerogel) of AC and blank alginate, i.e., A (without adding carbon to the alginate solution) were also prepared. These gels were named as AC alginate xerogel (ACX), AC alginate cryogel (ACC), AC alginate aerogel (ACA), alginate xerogel (AX), alginate cryogel (ALC), and alginate aerogel (AA).

2.4. Characterization of Adsorbents. The surface area of the gels was analyzed by Brunauer–Emmett–Teller (BET) analysis using a Belsorp Mini II, MicrotracBEL Corp., Japan. A thermogravimetric analyzer (TGA, Mettler Toledo Stare, Columbus) was used to study the thermal stability with a heating rate of 10 °C/min. Surface characteristics of the synthesized materials were examined using a field emission scanning electron microscope (FE-SEM, QUANTA FEG 450, FEI, Netherland) coupled with an energy dispersive X-ray (EDAX) analysis system for elemental composition. The crystallinity of the material was determined using a Rigaku (SmartLab SE) X-ray diffraction (XRD) system. The charge or ζ-potential of the adsorbent (for pH 2–12) was measured using a dynamic light scattering (DLS) approach using a Zetasizer Nano-ZSP, Malvern, U.K. The attenuated total reflectance–Fourier transform infrared (ATR-FTIR) spectra of gels were obtained using a Thermo Fischer (Nicolet, iS5) FTIR with a scanning range from 400 to 4000 cm^{-1}.

2.5. Selection of the Adsorbent. The performance of all prepared adsorbents (or gels) was checked by determining the removal percentage (%R) of the targeted HM, viz., Cr(VI), Hg(II), As(III), Pb(II), and Cd(II). An atomic absorption spectrometer (AAS, PerkinElmer, PinAAcle 900F) was used for the HM quantification. For the adsorption experiment, 2 g/L dose of each adsorbent was used for 4 ppm concentration of each targeted HM. The preliminary adsorption experiment was performed under constant conditions of pH 6, 30 °C temperature, and 60 min contact time. Among all adsorbents, %R of HMs was found to be higher by SLACC (activated carbon alginate cryogel from sweet lime), which was 100, 100, 100, 99.75, and 77.62% for Cr, Cd, Pb, Hg, and As, respectively (Table S1). Thus, SLACC was found to be the best adsorbent and thus used for further batch adsorption study.

2.6. Quality Control for AAS. Before the metal analysis, the atomic absorption spectrophotometer (AAS) was calibrated by standard reference materials (SRMs) of heavy metals. High correlation coefficient (R^2 > 0.99) values were obtained after running standards of heavy metals in triplicate. The analysis of each sample was done three times on the AAS followed by the blank sample to ensure the reliability of the produced data. Furthermore, the standards were also run at regular intervals while analyzing samples.

2.7. Batch Adsorption Experiment. First, the adsorption experiment was performed to determine the equilibrium time of adsorption. In this experiment, 2 g/L adsorbent (SLACC) was added to 4 ppm mix solution of Cr(VI), Pb(II), As(III), Hg(II), and Cd(II) at pH 6 and a temperature of 30 °C. This solution was agitated for time intervals ranging from 10 to 90 min using a Rota spin at 50 rpm. Sample analysis was done on an atomic absorption spectrometer. The proficiency of SLACC was judged on the basis of adsorption capacity (q_e) and removal percentage (%R) of heavy metals by it, which can be given by the following equations

$$q_e = \frac{(C_i - C_f)}{W} \times V \quad (1)$$

$$\%R = \frac{(C_i - C_f)}{C_i} \times 100 \quad (2)$$

where C_i and C_f are the initial and final concentrations of an analyte (in mg/L), q_e is the adsorption capacity in mg/g, and V and w are the volume of the solution (L) and weight of adsorbent (g), respectively.

3. RESULTS AND DISCUSSION

3.1. Characterization. Surface properties of adsorbents were inspected using a surface area analyzer. From the BET plot of SLACC represented by Figure 1, the surface area of SLACC was found to be 3.03 m^2/g, which is slightly lower than the BET surface area of SLAC (3.82 m^2/g). On the other hand, the blank alginate cryogel (ALC) has a low surface area (0.853 m^2/g) compared to that of SLAC (3.82 m^2/g) and SLACC (3.03 m^2/g), due to which it could not show much adsorption. Thus, the high surface area of SLACC facilitated the better adsorption of heavy metals.

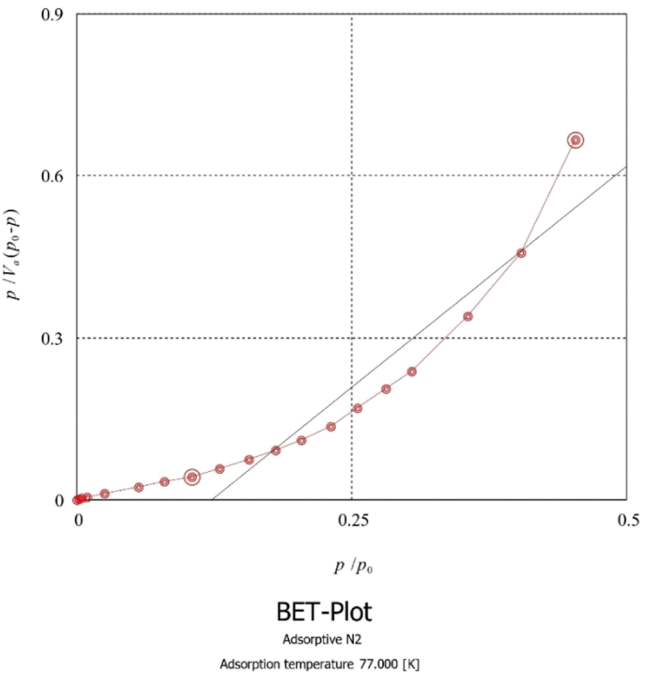

Figure 1. BET plot of SLAC.

The XRD spectra of SLAC and commercial activated carbon (AC) are presented in Figure 2a,b. High-intensity peaks in the XRD spectra of SLAC confirmed that the activated carbon prepared from sweet lime was crystalline, while the intensity of the peaks was very weak for AC. Therefore, on the basis of

https://doi.org/10.1021/acsomega.2c03786
ACS Omega 2022, 7, 41997–42011

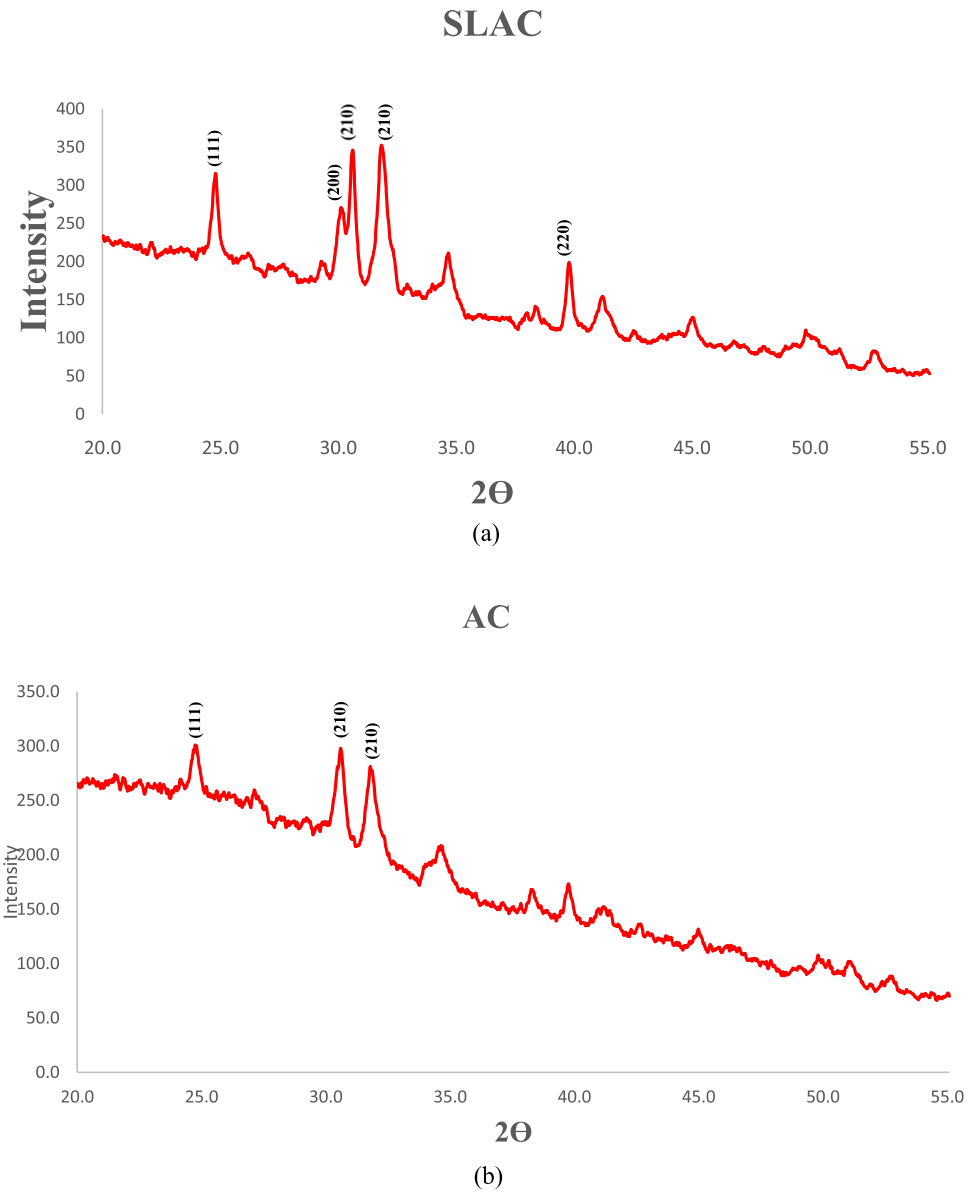

Figure 2. XRD spectra of SLAC (a) and commercial activated carbon (AC) (b).

diffraction peaks of XRD spectra, it became clear that SLAC was crystalline in nature.

The scanning electron microscopy (SEM) images of the blank alginate cryogel (ALC) and alginate cryogel of sweet lime-derived activated carbon (SLACC) are shown in Figure 3a,b, respectively. From Figure 3a, it can be seen that ALC has a smooth or planar surface with little cracks (due to freeze drying). On the other hand, SLACC (Figure 3b) has a rough surface due to impregnation of the sweet lime-derived activated carbon (SLAC) on SLACC. Moreover, the cracks and porosity of the SLACC were also increased by freeze drying that facilitated the adsorption of heavy metals. From the EDAX spectra (Figure 4), it can be seen that Ca was present in a high amount as compared to that of the blank alginate cryogel, i.e., ALC (EDAX of ALC is provided in Figure S1), which confirmed the replacement of Na ions by Ca during gel formation via crosslinking. The carbon content of SLACC was also found to be much higher, which ensured that SLAC has been impregnated on SLACC.

The FTIR spectra of the compounds were used to determine the presence of functional groups and the possible mechanism of interactions between the adsorbent and adsorbate. The scanning of spectra was done in the range of 4000−400 cm^{-1}. The FTIR spectra of the blank alginate cryogel (ALC), i.e., without carbon, sweet lime activated carbon (SLAC), sweet lime activated carbon cryogel (SLACC), and sweet lime activated carbon cryogel after adsorption of heavy metals are presented in Figure 5a−d, respectively. For ALC (Figure 5a), the broad peak obtained in the spectra at 3239 cm^{-1} was due to the −OH stretching vibration, while peaks at 1587, 1413, and 1024 cm^{-1} correspond to the asymmetric −COO stretching, symmetric −COO stretching, and −C−O−C− stretching, respectively.[18,27] For SLAC (Figure 5b), the −OH stretching band at 3383 cm^{-1} was observed. Bands at 2919 and 2850 cm^{-1} correspond to the aromatic and aliphatic −CH stretching, respectively, while the band at 2008 cm^{-1} could be due to the overtone from aromatic stretch or due to the −C≡C− stretching. The bands due to C−C bonds can be attributed to the formation of carbonaceous compounds due to pyrolysis.

https://doi.org/10.1021/acsomega.2c03786
ACS Omega 2022, 7, 41997−42011

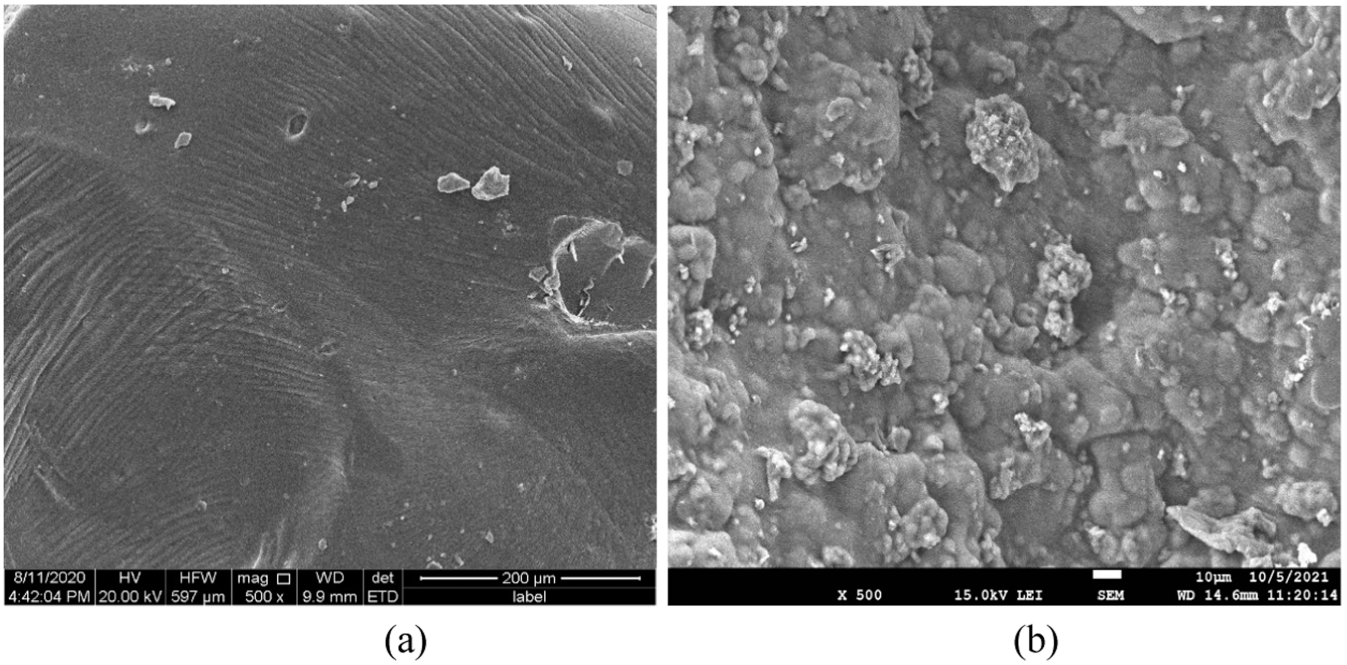

Figure 3. SEM images of ALC (a) and SLACC (b).

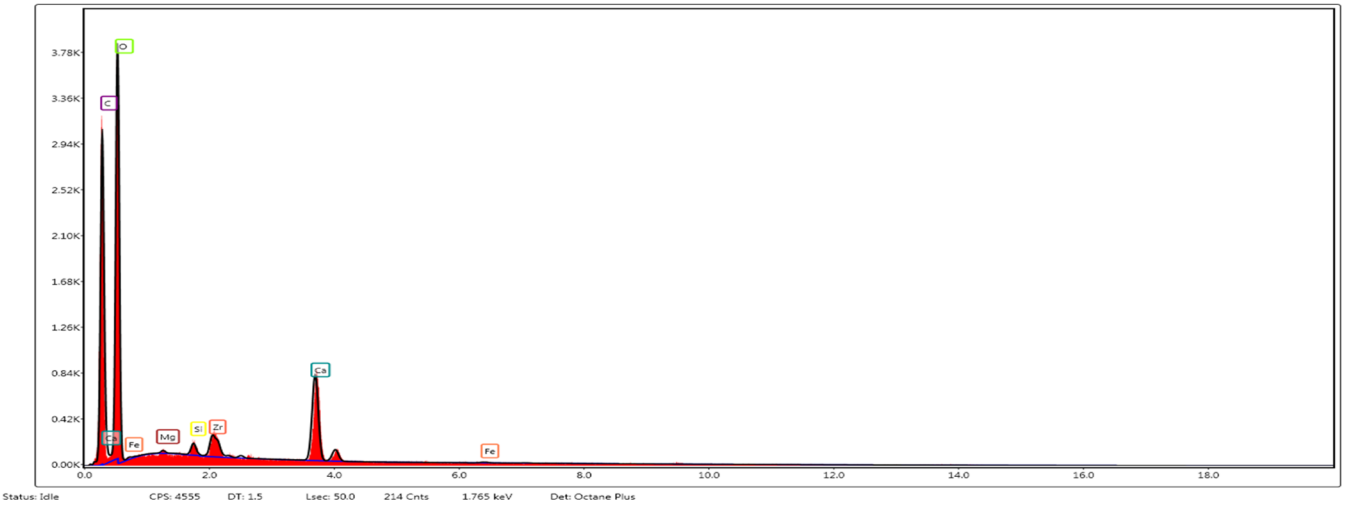

Figure 4. EDAX spectra of SLACC.

The band at 1621 cm^{-1} corresponds to the −COO group stretching. In SLACC (Figure 5c), the characteristic bands of −OH stretching (3261 cm^{-1}), −CH stretching (2000 cm^{-1}), −C═O (1650 cm^{-1}), and −COC− stretching (1028 cm^{-1}) were observed, suggesting that the dominant bands of ALC and SLAC were retained in SLACC. Figure 5d shows the FTIR spectra of SLACC after heavy metal adsorption. From the spectra, it was observed that the bands of −OH, −C═O, and −COC become weaker, which confirmed the interaction of these groups with heavy metal ions by coordination of −OH and −COO groups with heavy metals (chelation) that facilitated their adsorption.[28] The comparison of spectra is provided in Figure S2.

A thermogravimetric analyzer (TGA) was used to check the thermal stability of the adsorbent. The plot of weight percent of three materials (ALC, SLAC, and SLACC) with respect to temperature is shown in Figure 6. It can be seen that there was 20% weight loss of ALC from 25 to 200 °C and from 200 to 300 °C, a huge weight of ALC (50% weight loss) was lost, and then, its decomposition slowed down till 1000 °C. The weight loss pattern of SLAC shows that only 10% of its weight was lost from 25 to 200 °C and after 800 °C, 50% weight was lost, which suggested that it is highly stable. SLACC, which is a composite of ALC and SLAC, followed a similar pattern of weight loss as of ALC, but its stability was better than that of ALC as 60% weight of ALC was lost after 300 °C, while 50% weight of SLACC was lost after 300 °C. Thus, the TGA plot suggested that the stability of SLACC was improved after the addition of SLAC.

To measure the point of zero charge (pzc) of SLACC, it was dispersed in six solutions whose pH values were maintained at 2, 4, 6, 8, 10, and 12 with the help of 0.1 M HCl and 0.1 M NaOH. The potential of these six solutions was recorded using a Zetasizer. The graph between pH and zeta (ζ)-potential is presented in Figure 7. The calculated value of pzc from the graph was found to be 2.92, which signifies that SLACC is

https://doi.org/10.1021/acsomega.2c03786
ACS Omega 2022, 7, 41997−42011

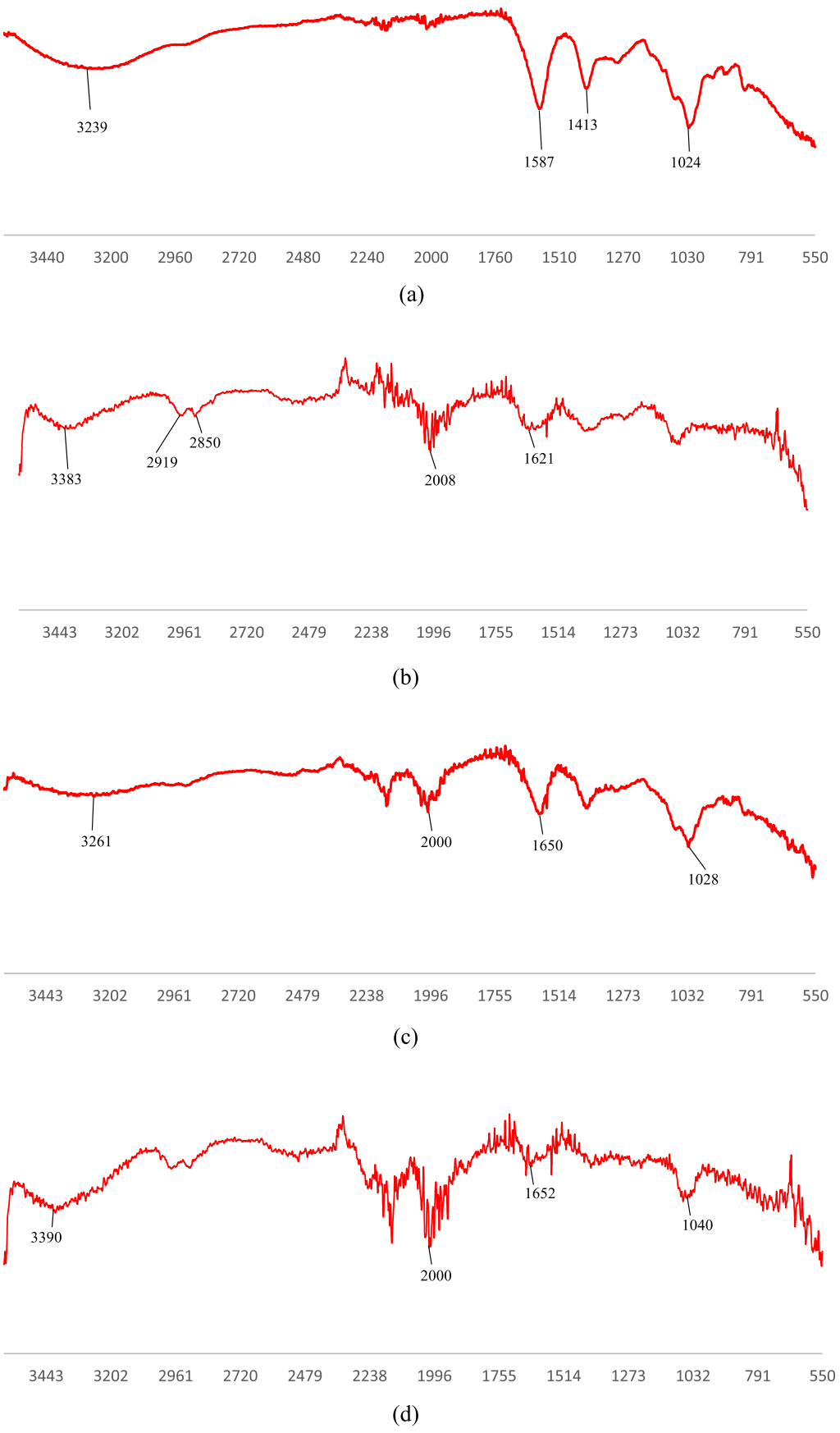

Figure 5. FTIR spectra of ALC (a), SLAC (b), SLACC before adsorption (c), and SLACC after adsorption (d).

https://doi.org/10.1021/acsomega.2c03786
ACS Omega 2022, 7, 41997−42011

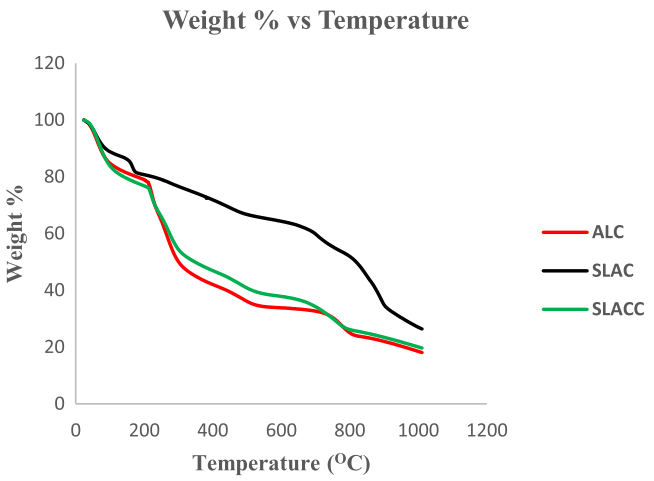

Figure 6. TGA plot of ALC, SLAC, and SLACC.

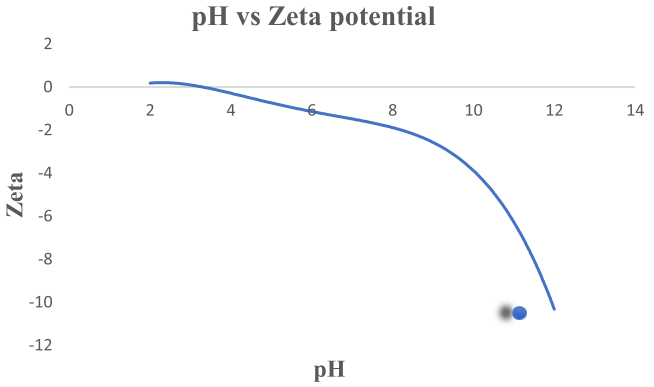

Figure 7. Zeta (ζ) potential of SLACC with respect to pH.

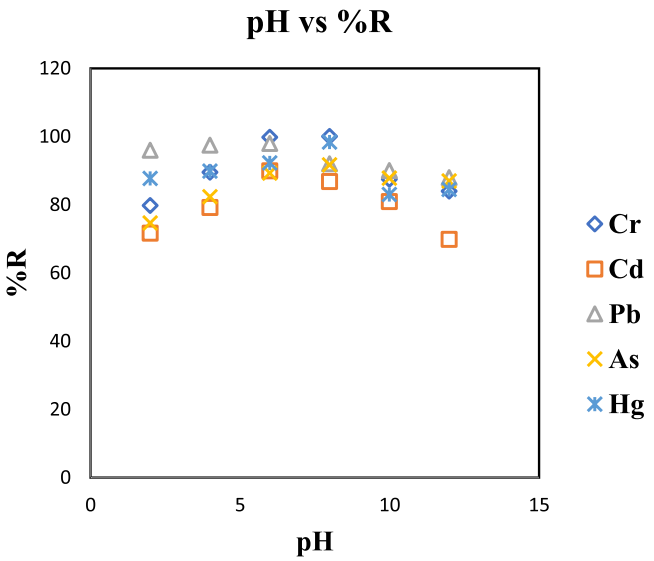

Figure 8. Effect of pH on %*R* of Cr, Cd, Pb, As, and Hg.

positively charged at pH below 2.92, neutrally charged at pH 2.92, and negatively charged at pH above 2.92. The uptake of positively charged metal ions by SLACC at pH 6 confirmed the electrostatic interactions between them that facilitated the adsorption. On the whole, SLACC was a negatively charged adsorbent whose ζ-potential values were negative at pH 4, 6, 8, 10, and 12.

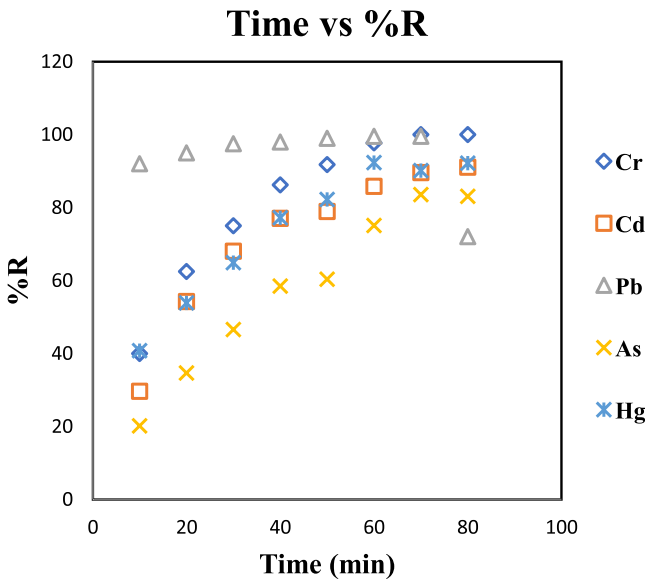

Figure 9. Effect of time on %*R* of Cr, Cd, Pb, As, and Hg.

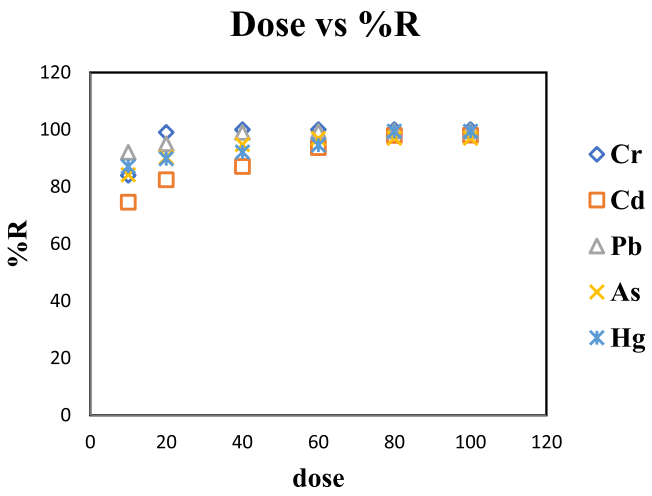

Figure 10. Effect of the adsorbent dose on %*R* of Cr, Cd, Pb, As, and Hg.

3.2. Factors Affecting the Adsorption of Heavy Metals. *3.2.1. Effect of pH.* pH is a significant factor in most of the chemical reactions, and in this study, pH played a key role in the adsorption of HM. From Figure 8, it can be seen that at low pH (pH 2−4), % removal of HMs is low. The % removal of these heavy metals increased with the increase in pH (pH 6−8) and again decreased with a further increase of pH. The decreased adsorption of heavy metals at low pH (pH < pzc) was mainly because of the increase in the H^+ concentration that resulted in the competition between positively charged metal ions and H^+ for binding with negatively charged functional groups (−OH and −COOH) of SLACC. As the pH increases (pH > pzc), the concentration of H^+ decreases, and thus, adsorption (more than 90% removal of heavy metals) occurs easily due to electrostatic attraction between the negatively charged SLACC surface and positively charged heavy metals. At higher pH, i.e., from pH 8 to 12, the OH^- concentration gets increased and the heavy metals get precipitated in the form of their hydroxides, which resulted in the decreased uptake of heavy metals by the surface sites of

https://doi.org/10.1021/acsomega.2c03786
ACS Omega 2022, 7, 41997−42011

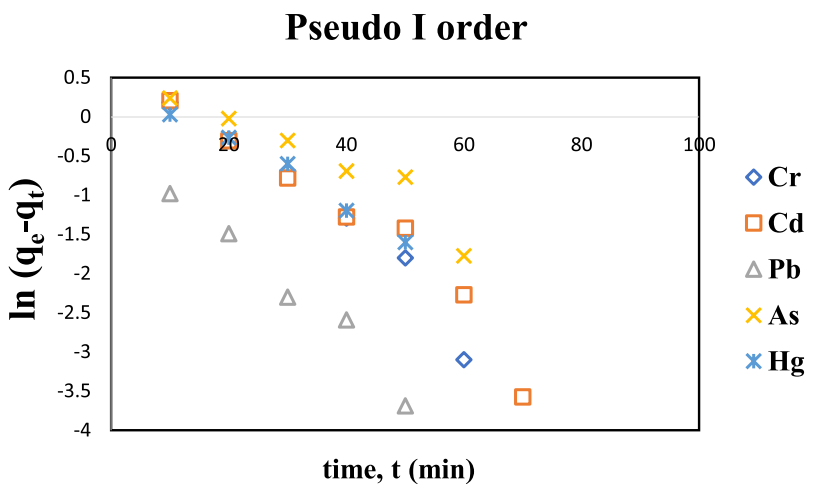

(a)

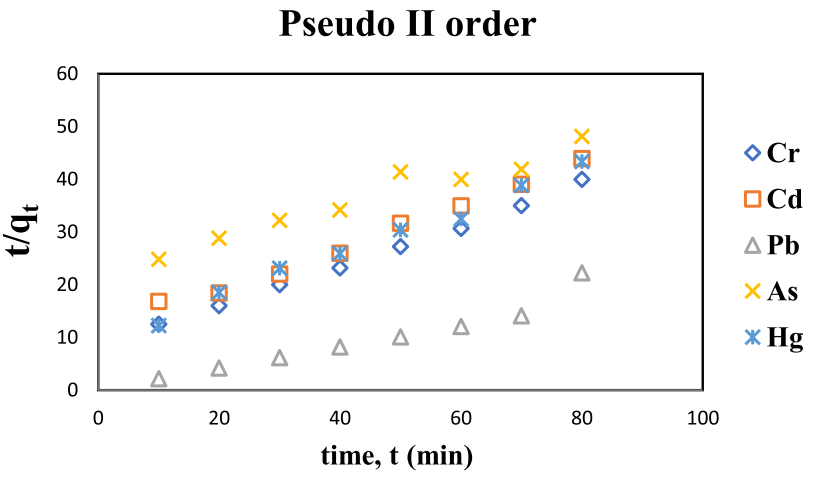

(b)

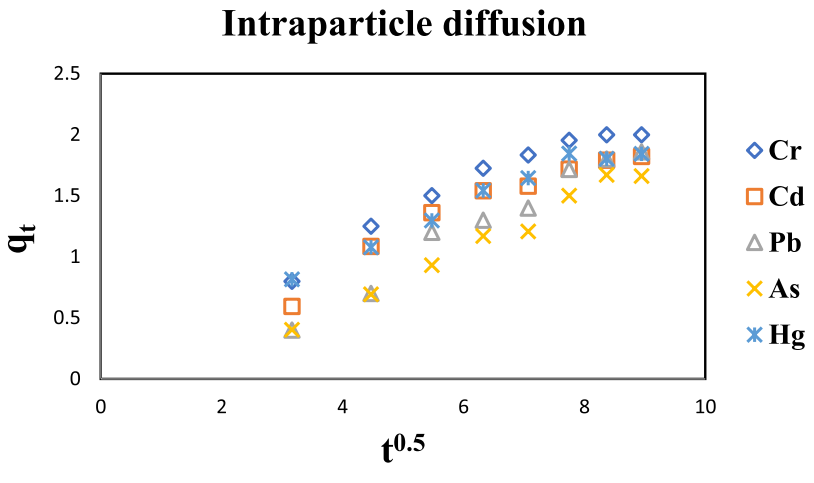

(c)

Figure 11. Kinetic models of pseudo-first order (a), pseudo-second order (b), and intraparticle diffusion (c).

SLACC. Similar results were obtained by Guo et al. to remove Pb(II) using biomass-derived activated carbon.[29]

3.2.2. Effect of Time. Time is an important parameter in the adsorption process. With regard to this, adsorption of Pb, Cr, Hg, Cd, and As was investigated at different time intervals ranging from 10 to 80 min. The adsorption was carried out with 4 ppm concentration of heavy metal solution to which a 20 mg dose of SLACC was used. Figure 9 shows the relation

https://doi.org/10.1021/acsomega.2c03786
ACS Omega 2022, 7, 41997−42011

Table 1. Parameters of Kinetic Modeling

I order			
heavy metals	q_{cal}	q_{exp}	R^2
Cr	2.69	2.00	0.951
Cd	2.52	1.82	0.937
Pb	0.77	4.97	0.971
As	2.04	1.67	0.910
Hg	1.70	1.84	0.984
II order			
heavy metals	q_{cal}	q_{exp}	R^2
Cr	2.59	2.00	0.997
Cd	2.49	1.82	0.989
Pb	5.06	4.97	1.000
As	3.24	1.67	0.952
Hg	2.38	1.84	0.989
IPD			
heavy metals	K_{id}	C	R^2
Cr	0.208	0.286	0.942
Cd	0.203	0.125	0.933
Pb	0.260	0.381	0.973
As	0.229	0.321	0.984
Hg	0.224	0.091	0.995

between the removal percentage of heavy metals with time. It was observed that except As, other heavy metals (Cr, Cd, Pb, and Hg) were removed to more than 50% of their initial concentration. It was seen that 92% of Pb was removed in 10 min while in 60 min, all metals (including As) were removed to more than 75%. Equilibrium was achieved within 60 min for Cr, Pb, and Hg and within 70 min for As and Cd. The adsorption of HMs was increased as the time of residence or contact between the adsorbate and adsorbent was increased. Once the equilibrium is achieved, the rate of adsorption decreased as the number of active sites of the adsorbent was reduced.

3.2.3. Effect of Dose. For observing the effect of the dose on the extent of HM adsorption, different dosages of the adsorbent SLACC (from 10 to 100 mg) were used. The adsorption was carried out with 4 ppm initial concentration of heavy metals at pH 6 with 60 min contact time with the adsorbent. It was observed that in a 20 mg dose, around 90% of Cr, Pb, Hg, and As was removed except Cd (82.45% removed). The adsorption was increased with the increase in the dose due to the increased number of metal binding active sites. The percentage removal of heavy metals was almost similar for 80 and 100 mg doses, where more than 97% removal of heavy metals was observed, which suggested that a 80 mg dose of SLACC was optimum for the maximum adsorption (Figure 10).

3.3. Kinetics of Adsorption. Kinetic modeling of adsorption is necessary for understanding the adsorption mechanism. It is useful in the determination of the diffusion rate of the HM from its solution to the adsorbent.[30] In this study, kinetic data were fitted on the following models

3.3.1. Pseudo-First-Order Model. A linear form of the pseudo-first-order model is given by the following equation[31]

$$\ln(q_e - q_t) = \ln q_e - K_1 t \quad (3)$$

where t is the time of adsorption, q_t is the adsorption capacity at time t, q_e is the adsorption capacity at equilibrium, and K_1 is first-order rate constant. In this, the graph is plotted between $\ln(q_e - q_t)$ and t.

3.3.2. Pseudo-Second-Order Model. The equation for this model is given by[32]

$$\frac{t}{q_t} = \frac{1}{K_2 q_e^2} + \frac{t}{q_e} \quad (4)$$

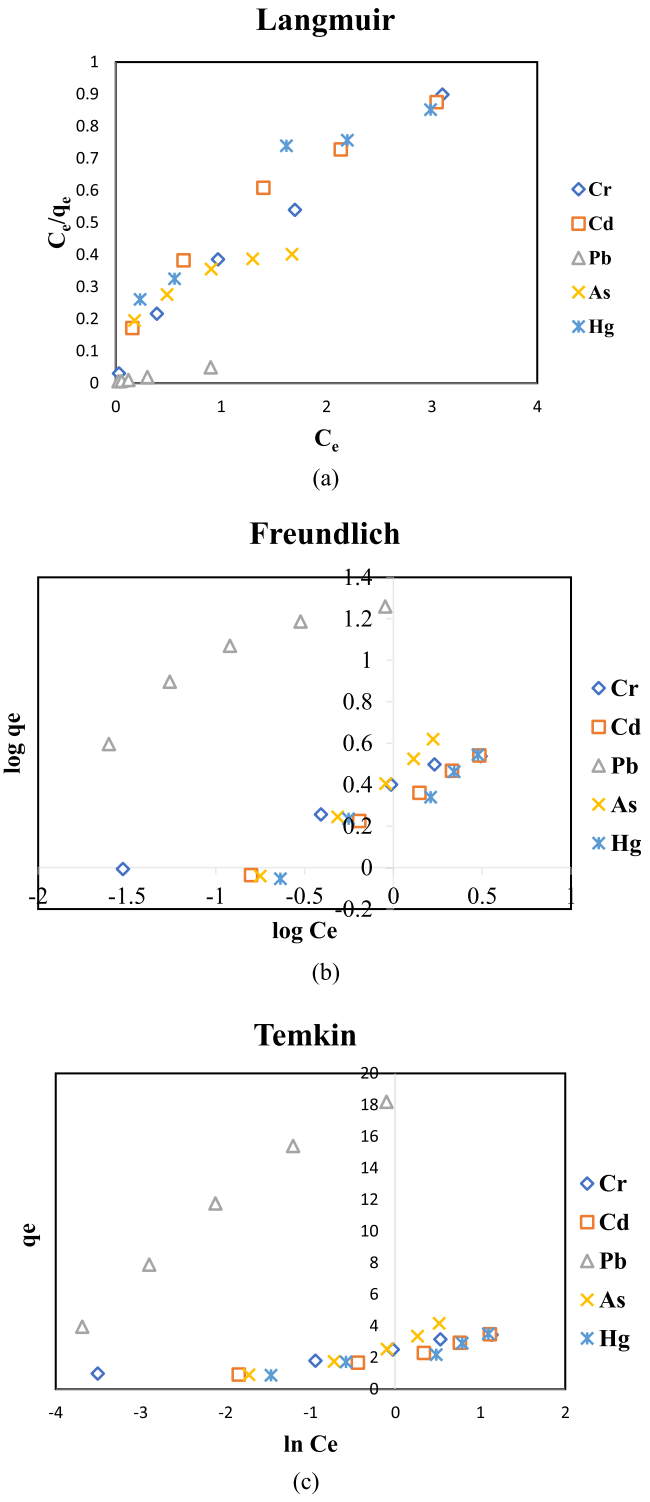

Figure 12. Adsorption isotherm models of Langmuir (a), Freundlich (b), and Temkin (c).

https://doi.org/10.1021/acsomega.2c03786
ACS Omega 2022, 7, 41997−42011

Table 2. Parameters of Adsorption Isotherm Modeling

Langmuir			
heavy metals	q_m	K	R^2
Cr	3.71	3.35	0.985
Cd	4.22	1.16	0.956
Pb	20.04	11.09	0.999
As	7.31	0.68	0.907
Hg	4.37	0.95	0.916
Freundlich			
heavy metals	n	K_f	R^2
Cr	3.58	2.54	0.988
Cd	2.24	2.06	0.997
Pb	2.43	22.87	0.892
As	1.50	2.84	0.997
Hg	2.02	1.96	0.958
Temkin			
heavy metals	b	A	R^2
Cr	4.70	149.49	0.936
Cd	3.02	15.33	0.944
Pb	0.62	127.61	0.981
As	1.82	9.03	0.932
Hg	2.72	10.61	0.928

Table 3. Thermodynamic Parameters for Adsorption

heavy metals	ΔH	ΔS	ΔG	temp (K)
chromium	1622.56	98.09	−4971.04	293
			−13 334.6	303
			−21 582.8	313
cadmium	59 956.41	212.80	−2370.63	293
			−4572.97	303
			−6623.31	313
lead	36 975.68	133.47	−7741.75	293
			−9229.03	303
			−10 407.1	313
arsenic	74 408.63	262.12	−2500.72	293
			−4785.45	303
			−7758.35	313
mercury	46 580.01	172.93	−4568.97	293
			−4788.14	303
			−8095.43	313

where k_2 is the second-order rate constant. The graph is plotted between $\frac{t}{q_t}$ and t.

3.3.3. Intraparticle Diffusion Model. This model is used for the determination of the rate-determining step in aqueous systems. A linear form of Weber and Morris' intraparticle diffusion model can be given by[33]

$$q_t = K_{id} t^{0.5} + C \quad (5)$$

where K_{id} is the intraparticle diffusion rate constant (mg/(g $\text{min}^{0.5}$)), $t^{0.5}$ is the adsorption half-life, and C is the intercept that can be evaluated from the slope of the plot between q_t and $t^{0.5}$. For this, the graph is plotted between q_t and $t^{0.5}$.

The kinetic isotherms were applied by checking adsorption in different time intervals (from 10 to 80 min), for which the initial concentration of heavy metals was 4 ppm, while the adsorbent dose was 20 mg. The graph of these three adsorption isotherms is presented in Figure 11a−c, respectively. The parameters obtained on the basis of these plots are listed in Table 1.

The best fitting of the kinetic model depends on the R^2 values. Among the three kinetic models, the pseudo-second-order model had the high R^2 values in comparison to the pseudo-first-order and intraparticle diffusion models. From the plot of the pseudo-second-order model, the calculated adsorption capacities (q_{cal}) for Cr, Cd, Pb, As, and Hg were found to be 2.59, 2.49, 5.06, 3.24, and 2.38 mg/g, respectively. These adsorption capacities were similar to the experimental adsorption capacities (q_{exp}) listed in Table 1, suggesting that the adsorption followed the pseudo-second-order kinetics and chemisorption is taking place. The intraparticle diffusion model helped determine whether the adsorption is governed by mass transport of the solute from the liquid phase to the solid phase or by the intraparticle diffusion of the solute onto the gel. This phenomenon was studied by plotting a graph between the amount of HM adsorbed at time t and the square root of time. The graph of IPD (Figure 11c) can be divided into two parts, in which the linear part indicated the diffusion of the HM to the gel, while the curved part indicated the boundary layer effect. Low values of intercept C suggested a lower boundary effect, implying that intraparticle diffusion is more dominant.[34]

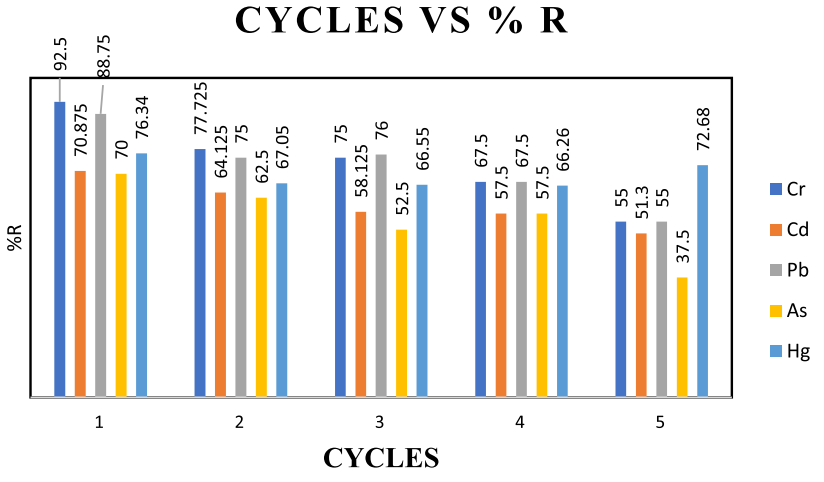

Figure 13. Percentage removal of heavy metals with respect to regeneration cycles.

https://doi.org/10.1021/acsomega.2c03786
ACS Omega 2022, 7, 41997−42011

Table 4. Concentration of Element Leaching from Adsorbents

	concentration of metals in mg/L									
adsorbent	Cr	Cd	Pb	Hg	As	Na	K	Mg	Zn	Ca
ALC	ND[a]	ND	ND	ND	ND	0.466	0.114	ND	0.023	3.511
AC	ND	ND	ND	ND	0.13	0.082	0.094	ND	ND	ND
SLAC	ND	ND	ND	ND	ND	0.040	0.232	ND	ND	ND
SLACC	ND	ND	ND	ND	ND	0.039	ND	ND	ND	1.481

[a]ND—not detected.

Table 5. Percentage Removal (%R) of Heavy Metals from Real Samples of Water

	%R				
sample name	Cr	Cd	Pb	As	Hg
R1	96.61	89.01	88.80	91.87	89.81
R2	96.41	92.04	83.57	90.81	91.01
R3	96.13	92.03	87.45	83.33	87.40
R4	97.11	89.02	84.65	89.84	89.31
R5	94.91	92.55	89.34	87.11	82.40
R6	96.66	91.35	90.85	89.45	86.65
R7	94.91	92.59	92.00	92.67	94.28
R8	95.57	89.24	94.22	82.81	86.45
R9	97.76	92.03	91.13	86.92	94.24
R10	93.92	90.00	82.50	88.21	87.46
R11	95.76	92.04	84.09	91.11	88.84
R12	95.17	91.45	92.65	90.83	96.49
R13	95.00	91.14	90.23	81.67	88.66
R14	95.61	92.27	89.34	90.42	93.35
R15	98.07	89.58	86.67	89.84	85.46

Table 6. Percentage Removal (%R) of Other Metals from Real Samples of Water

	%R				
sample name	Na	K	Mg	Zn	Ca
R1	3.84	22.17	31.53	4.71	35.75
R2	6.92	23.69	12.66	10.75	33.00
R3	15.33	28.54	21.53	8.65	28.40
R4	9.84	19.24	27.69	2.64	31.88
R5	18.41	21.74	18.84	2.90	24.76
R6	33.36	21.42	25.26	18.59	31.96
R7	18.43	21.29	0.00	16.47	28.72
R8	1.51	28.86	14.90	2.52	19.95
R9	10.93	27.00	1.08	12.59	18.80
R10	11.53	16.19	14.28	8.79	24.51
R11	0.00	26.96	12.34	33.10	34.63
R12	7.45	22.94	8.88	5.26	33.82
R13	50.15	23.60	26.53	27.73	20.65
R14	0.00	24.98	7.00	20.06	28.69
R15	3.11	22.34	11.84	26.42	19.24

3.4. Isotherms of Adsorption. Modeling of adsorption data of five HMs on the gel under optimal conditions of temperature, pH, and contact time was studied with the help of the following models.[15]

3.4.1. Langmuir Adsorption Isotherm. This isotherm is based on the monolayer adsorption, assuming the surface of the adsorbent to be homogeneous without any adsorbate−adsorbate interaction.[35] Its equation can be given as

$$\frac{C_e}{q_e} = \frac{C_e}{q_m} + \frac{1}{K_a q_m} \quad (6)$$

where C_e is the equilibrium concentration, q_m is the maximum adsorption capacity, q_e is the adsorption capacity at equilibrium, and K_a is Langmuir's constant.

The separation factor (R_L) of the Langmuir model can be given as

$$R_L = \frac{1}{1 + K_a C_e} \quad (7)$$

where K_a is the affinity constant or Langmuir's constant and C_e is equilibrium concentration. For favorable adsorption, R_L should range from 0 to 1.

3.4.2. Freundlich Adsorption Isotherm. According to this isotherm, the surface of the adsorbent is considered heterogeneous. Its equation can be given as[36]

$$\log q_e = \log K_f + \frac{1}{n} \log C_e \quad (8)$$

where q_e is the adsorption capacity of the adsorbent, K_f is the Freundlich adsorption coefficient, C_e is the equilibrium concentration of the solution, and n is the exponential coefficient.

3.4.3. Temkin Adsorption Isotherm. The linear form of the Temkin adsorption equation can be expressed as[37]

$$q_e = \frac{RT}{b} \ln A + \frac{RT}{b} \ln C_e \quad (9)$$

where R is the gas constant, T is the temperature, A and b are the Temkin constants.

The adsorption isotherms were applied with the initial concentration of heavy metals ranging from 2 to 10 ppm. The contact time for adsorption was 60 min with a 20 mg dose of the adsorbent. The graphs of these three adsorption isotherms are represented in Figure 12a−c. The parameters obtained on the basis of these plots are listed in Table 2.

For the Langmuir isotherm, maximum adsorption capacities (q_m) of the adsorbent for Cr, Cd, Pb, As, and Hg were found to be 3.71, 4.22, 20.04, 7.31, and 4.37 mg/g, respectively. The values of the separation factor (R_L) were lying between 0 and 1 (Table S2), suggesting the favorable adsorption. From the Freundlich isotherm, the values of n were found to be 3.58, 2.24, 2.43, 1.50, and 2.02 for Cr, Cd, Pb, As, and Hg, respectively, which were in accordance with the progression of adsorption.[38] From the Temkin model, low values of heat of adsorption, i.e., 4.70, 3.02, 0.62, 1.82, and 2.72 for Cr, Cd, Pb, As, and Hg, respectively, suggested highly favorable adsorption.[39] Among the three models (Langmuir, Freundlich, and Temkin), the data were best fitted to the Freundlich isotherm (having higher R^2 values), suggesting the adsorption of ions on the heterogeneous surface via adsorbate−adsorbent interactions.[36]

https://doi.org/10.1021/acsomega.2c03786
ACS Omega 2022, 7, 41997−42011

Table 7. Adsorption of Heavy Metals by Different Adsorbents

s. no.	adsorbent	adsorbate	adsorption capacity (q) in (mg/g)	references
1	buffalo weed biochar alginate beads	Cd(II)	9.73	40
2	alginate−chitosan beads	Cd(II)	6.63	41
3	poly(vinyl alcohol)−alginate gel	Pb(II)	0.60	42
4	iron oxide-derived alginate gel	As(V)	0.0226	43
5	alginate−montmorillonite/polyaniline nanocomposite	Cr(VI)	29.89	44
6	alginate gelatin biopolymeric beads	Cr(VI)	0.833	45
7	alginate−Ayous wood sawdust	Cd(II)	6.21	46
8	mosambi (*Citrus limetta*) peel dust	Cr(VI)	3.623	47
9	magnetic alginate beads	Cr(VI)	14.29	48
10	Fe_3O_4−MnO_2−alginate xerogel	Cr(II) and Cd(II)	7.24 and 7.79	1
11	alginate cryogel of sweet lime-derived activated carbon (SLACC)	Cr(VI), Cd(II), Pb(II), Hg(II) and As(III)	3.71, 4.22, 20.04, 4.37 and 7.31	this work

3.5. Thermodynamics of Adsorption. The thermodynamic study was done in this work with the help of Gibbs and van't Hoff equations that can be given as

$$\Delta G = -RT \ln K_0 \quad (10)$$

$$K_0 = C_a/C_S \quad (11)$$

$$\Delta G = \Delta H - T\Delta S \quad (12)$$

where ΔH is the enthalpy change, T is the temperature change, ΔS is the entropy change, ΔG is the Gibbs free energy, R is the gas constant, K_0 is the equilibrium constant, C_a is the concentrations of the adsorbate on the adsorbent, and C_S is the concentration of the adsorbate in solution. From the van't Hoff plot, values of thermodynamic parameters (ΔH, ΔS, and ΔG) of for all five heavy metals were obtained and are listed in Table 3. The positive values of enthalpy change (ΔH) showed that the adsorption was endothermic in nature, which was also supported by the increased adsorption of HM with increasing temperature from 293 to 313 K. Positive values of entropy change (ΔS) indicated the randomness of adsorption, while negative values of Gibbs free energy (ΔG) showed that the adsorption phenomenon was spontaneous, which in turn became more negative with the increase of temperature. Thus, thermodynamic study revealed that the adsorption was spontaneous and endothermic in nature.

3.6. Regeneration and Reuse of the Adsorbent. The reusability of the adsorbent SLACC was checked once used for the adsorption first time. The isolated adsorbent was washed or regenerated using 0.1 M EDTA, dried, and used again for the adsorption of heavy metals from their 4 ppm aqueous solution. This adsorption was termed as the first cycle, and in this study, the performance of the adsorbent was checked for five cycles. Figure 13 presents the percentage removal of heavy metals for five cycles. It was seen that more than 70% removal of HMs was achieved in the first cycle, in which 92.5% of Cr was removed. The %R of HMs decreased with each cycle because of the reduced number of active sites, and it was further decreased to 60% after the fourth cycle. After the fifth cycle, except As, more than 50% of HMs were removed, in which the %R of Hg was maximum (72.68%). The reusability of the adsorbent showed that it is economical and environment-friendly.

3.7. Leaching Study. The leaching study was done for the assessment of the adsorbents' toxicity. The study was used to observe the release of toxic elements from adsorbents when in contact with aqueous solution. The leaching of the elements Cr, Cd, Pb, Hg, As, Na, K, Mg, Zn, and Ca was observed from the adsorbents ALC, AC, SLAC, and SLACC. For this experiment, 100 mg of each adsorbent (ALC, AC, SLAC, and SLACC) was added to separate flasks containing 20 mL of water. The flask was agitated at 100 rpm for 24 h. After that, the materials were isolated, and these water samples were analyzed on AAS for metals. The concentrations of the leached elements are given in Table 4. It can be seen that high amounts of Na, K, and Ca were leached from ALC, while lower amounts of As, Na, and K were leached from commercial activated carbon (AC) and SLAC. From SLACC, low amounts of Na and Ca were leached into water, but their concentrations were within their permissible limits. Therefore, SLACC was found to be the safe adsorbent for water remediation from toxic heavy metals.

3.8. Application in Real Samples. The adsorption of the targeted heavy metals (Cr, Pb, Hg, As, and Cd) and essential metals was checked in real samples of water, which were collected from 15 different sites (R1−R15) of the river Gomti, Lucknow (Table S3). Removal percentages of heavy metals from these samples by SLACC are listed in Table 5. The adsorption was done in the same way as the batch experiment was conducted. Briefly, 20 mg of the adsorbent SLACC was used for a 20 mL water sample and agitated at 50 rpm for 60 min. It can be seen that 80−97% of heavy metals were adsorbed by SLACC. Out of the five targeted metals, the %R of Cr was the highest (more than 90% of Cr was removed from all samples).

The adsorption of the essential elements (Na, K, Mg, Zn, and Ca) was also checked on the basis of %R, the values of which are presented in Table 6. It was observed that there was very minimal adsorption of Na, K, Mg, and Zn, while Ca was slightly better adsorbed probably due to its large size but much lesser adsorbed in comparison to the five targeted heavy metals. This confirmed that SLACC has high selectivity for Cr, Cd, Pb, As, and Hg, while other elements do not interfere in their adsorption.

4. CONCLUSIONS

In this study, activated carbons from the peels of banana and sweet lime were prepared. Their respective activated carbons were fused with alginate and dried in three ways, viz., air drying, freeze drying, and supercritical drying to get xerogels, cryogels, and aerogels, respectively. These gels were employed for the removal or adsorption of heavy metals (Cd, Pb, Cr, As, and Hg) from their aqueous solution. Among all the

https://doi.org/10.1021/acsomega.2c03786
ACS Omega 2022, 7, 41997−42011

adsorbents, SLACC (alginate cryogel of sweet lime-derived activated carbon) showed the highest removal percentage of heavy metals and thus was used for the batch study. Techniques such as SEM, EDAX, BET, TGA, XRD, and FTIR and a Zetasizer were used for characterizing the adsorbents. The effects of time, temperature, pH, adsorbent dose, and adsorbate concentrations on heavy metal adsorption were checked. The kinetic study followed the pseudo-second-order model, while the adsorption isotherm followed the Freundlich model. On the basis of the thermodynamic study, the adsorption was found to be spontaneous and endothermic. Furthermore, the adsorbent was also used on real water samples and showed up to 90% removal efficiency of the targeted heavy metals (Cr, Cd, Pb, Hg, and As). It was also seen that no toxic elements had leached from SLACC into water, making it an eco-friendly adsorbent. Further, SLACC showed multi element adsorption compared to other adsorbents (Table 7).

■ ASSOCIATED CONTENT

Supporting Information

The Supporting Information is available free of charge at https://pubs.acs.org/doi/10.1021/acsomega.2c03786.

EDAX spectra of ALC; FTIR spectra of ALC, SLAC, SLACC before adsorption, and SLACC after adsorption; percentage removal of heavy metals by different gels; separation factor (R_L) values of each heavy metal; and concentration of heavy metals before and after the addition of SLACC in real samples (PDF)

■ AUTHOR INFORMATION

Corresponding Authors

Nasreen G. Ansari − *Analytical Chemistry Laboratory, Regulatory Toxicology Group, CSIR-Indian Institute of Toxicology Research (CSIR-IITR), Lucknow 226001 Uttar Pradesh, India; Academy of Scientific and Innovative Research (AcSIR), Ghaziabad 201002, India;* orcid.org/0000-0003-3495-2360; Email: nasreen@iitr.res.in

Devendra K. Patel − *Analytical Chemistry Laboratory, Regulatory Toxicology Group, CSIR-Indian Institute of Toxicology Research (CSIR-IITR), Lucknow 226001 Uttar Pradesh, India; Academy of Scientific and Innovative Research (AcSIR), Ghaziabad 201002, India;* orcid.org/0000-0002-0168-9132; Email: dkpatel@iitr.res.in

Authors

Aditya Kumar − *Analytical Chemistry Laboratory, Regulatory Toxicology Group, CSIR-Indian Institute of Toxicology Research (CSIR-IITR), Lucknow 226001 Uttar Pradesh, India; Academy of Scientific and Innovative Research (AcSIR), Ghaziabad 201002, India*

Triparna Das − *Analytical Chemistry Laboratory, Regulatory Toxicology Group, CSIR-Indian Institute of Toxicology Research (CSIR-IITR), Lucknow 226001 Uttar Pradesh, India; Academy of Scientific and Innovative Research (AcSIR), Ghaziabad 201002, India*

Ravindra Singh Thakur − *Analytical Chemistry Laboratory, Regulatory Toxicology Group, CSIR-Indian Institute of Toxicology Research (CSIR-IITR), Lucknow 226001 Uttar Pradesh, India; Academy of Scientific and Innovative Research (AcSIR), Ghaziabad 201002, India;* orcid.org/0000-0001-8285-1797

Zeenat Fatima − *Analytical Chemistry Laboratory, Regulatory Toxicology Group, CSIR-Indian Institute of Toxicology Research (CSIR-IITR), Lucknow 226001 Uttar Pradesh, India*

Satgur Prasad − *Analytical Chemistry Laboratory, Regulatory Toxicology Group, CSIR-Indian Institute of Toxicology Research (CSIR-IITR), Lucknow 226001 Uttar Pradesh, India*

Complete contact information is available at: https://pubs.acs.org/10.1021/acsomega.2c03786

Author Contributions

[§]N.G.A. and D.K.P. contributed equally to this work. A.K.—methodology, experiment designing, data curation, and writing. T.D.—review and editing. R.S.T.—review and editing. Z.F.—sample preparation. S.P.—formal analysis and data curation. N.G.A. and D.K.P.—conceptualization, supervision, resources, writing, review, and editing.

Funding

Council of Scientific and Industrial Research (CSIR), India.

Notes

The authors declare no competing financial interest.

■ ACKNOWLEDGMENTS

The authors would like to acknowledge the Director, CSIR-Indian Institute of Toxicology Research, Lucknow, India, for supporting this work. The authors thank Dr. Satyakam Patnaik, Dr. Alok K. Pandey, and Dr. Sandeep Sharma for providing instrumental facilities of XRD, BET, TGA, Zetasizer, and ATR-FTIR. The Birbal Sahni Institute of Palaeosciences (BSIP), Lucknow, deserves special mention for providing the facility of SEM-EDAX. The authors would also like to thank Mohd. Muzammil and Rahul Verma for providing help in sample preparations and instrumental analysis.

■ ABBREVIATIONS

SLACC, alginate gel of activated carbon derived from sweet lime; AC, alginate cryogel; ppm, parts per million; %*R*, percentage removal

■ REFERENCES

(1) Kumar, A.; Prasad, S.; Saxena, P. N.; Ansari, N. G.; Patel, D. K. Synthesis of an Alginate-Based Fe3O4−MnO2 Xerogel and Its Application for the Concurrent Elimination of Cr(VI) and Cd(II) from Aqueous Solution. *ACS Omega* **2021**, *6*, 3931−3945.

(2) Nies, D. H. Microbial heavy-metal resistance. *Appl. Microbiol. Biotechnol.* **1999**, *51*, 730−750.

(3) Hegazi, H. A. Removal of heavy metals from wastewater using agricultural and industrial wastes as adsorbents. *HBRC J.* **2013**, *9*, 276−282.

(4) Rahman, Z.; Singh, V. P. The relative impact of toxic heavy metals (THMs) (arsenic (As), cadmium (Cd), chromium (Cr)(VI), mercury (Hg), and lead (Pb)) on the total environment: an overview. *Environ. Monit. Assess.* **2019**, *191*, No. 419.

(5) Biswas, S.; Sen, T. K.; Yeneneh, A. M.; Meikap, B. C. Synthesis and characterization of a novel Ca-alginate-biochar composite as efficient zinc (Zn2+) adsorbent: Thermodynamics, process design, mass transfer and isotherm modeling. *Sep. Sci. Technol.* **2019**, *54*, 1106−1124.

(6) Ayub, S.; Ali, S.; Khan, N.; Rao, R. Treatment of wastewater by agricultural waste. *Environ. Prot. Control J.* **1998**, *2*, 5−8.

(7) Liang, J.; Liu, J.; Yuan, X.; Zeng, G.; Yuan, Y.; Wu, H.; Li, F. A method for heavy metal exposure risk assessment to migratory

herbivorous birds and identification of priority pollutants/areas in wetlands. *Environ. Sci. Pollut. Res.* **2016**, *23*, 11806−11813.
(8) Rana, S. V. S. Perspectives in Endocrine Toxicity of Heavy Metals—A Review. *Biol. Trace Elem. Res.* **2014**, *160*, 1−14.
(9) Abraham, M. R.; Susan, T. B. Water contamination with heavy metals and trace elements from Kilembe copper mine and tailing sites in Western Uganda; implications for domestic water quality. *Chemosphere* **2017**, *169*, 281−287.
(10) Orlowski, C.; Piotrowski, J. K. Biological levels of cadmium and zinc in the small intestine of non-occupationally exposed human subjects. *Hum. Exp. Toxicol.* **2003**, *22*, 57−63.
(11) Anastopoulos, I.; Kyzas, G. Z. Composts as Biosorbents for Decontamination of Various Pollutants: a Review. *Water, Air, Soil Pollut.* **2015**, *226*, No. 61.
(12) Joseph, L.; Jun, B.-M.; Flora, J. R. V.; Park, C. M.; Yoon, Y. Removal of heavy metals from water sources in the developing world using low-cost materials: A review. *Chemosphere* **2019**, *229*, 142−159.
(13) Abdel Salam, O. E.; Reiad, N. A.; ElShafei, M. M. A study of the removal characteristics of heavy metals from wastewater by low-cost adsorbents. *J. Adv. Res.* **2011**, *2*, 297−303.
(14) Kadirvelu, K.; Thamaraiselvi, K.; Namasivayam, C. Removal of heavy metals from industrial wastewaters by adsorption onto activated carbon prepared from an agricultural solid waste. *Bioresour. Technol.* **2001**, *76*, 63−65.
(15) Abdelhafez, A. A.; Li, J. Removal of Pb(II) from aqueous solution by using biochars derived from sugar cane bagasse and orange peel. *J. Taiwan Inst. Chem. Eng.* **2016**, *61*, 367−375.
(16) Kobya, M.; Demirbas, E.; Senturk, E.; Ince, M. Adsorption of heavy metal ions from aqueous solutions by activated carbon prepared from apricot stone. *Bioresour. Technol.* **2005**, *96*, 1518−1521.
(17) Park, H. G.; Kim, T. W.; Chae, M. Y.; Yoo, I.-K. Activated carbon-containing alginate adsorbent for the simultaneous removal of heavy metals and toxic organics. *Process Biochem.* **2007**, *42*, 1371−1377.
(18) Hassan, A. F.; Abdel-Mohsen, A. M.; Elhadidy, H. Adsorption of arsenic by activated carbon, calcium alginate and their composite beads. *Int. J. Biol. Macromol.* **2014**, *68*, 125−130.
(19) Martinsen, A.; Skjåk-Bræk, G.; Smidsrød, O. Alginate as immobilization material: I. Correlation between chemical and physical properties of alginate gel beads. *Biotechnol. Bioeng.* **1989**, *33*, 79−89.
(20) Lin, S.; Huang, R.; Cheng, Y.; Liu, J.; Lau, B. L. T.; Wiesner, M. R. Silver nanoparticle-alginate composite beads for point-of-use drinking water disinfection. *Water Res.* **2013**, *47*, 3959−3965.
(21) Job, N.; Théry, A.; Pirard, R.; Marien, J.; Kocon, L.; Rouzaud, J.-N.; Béguin, F.; Pirard, J.-P. Carbon aerogels, cryogels and xerogels: Influence of the drying method on the textural properties of porous carbon materials. *Carbon* **2005**, *43*, 2481−2494.
(22) Uyar, G.; Kaygusuz, H.; Erim, F. B. Methylene blue removal by alginate−clay quasi-cryogel beads. *React. Funct. Polym.* **2016**, *106*, 1−7.
(23) Zhang, X.; Zhou, J.; Zheng, Y.; Wei, H.; Su, Z. Graphene-based hybrid aerogels for energy and environmental applications. *Chem. Eng. J.* **2021**, *420*, No. 129700.
(24) Barreca, S.; Orecchio, S.; Pace, A. The effect of montmorillonite clay in alginate gel beads for polychlorinated biphenyl adsorption: Isothermal and kinetic studies. *Appl. Clay Sci.* **2014**, *99*, 220−228.
(25) Plieva, F. M.; Karlsson, M.; Aguilar, M.-R.; Gomez, D.; Mikhalovsky, S.; Galaev', I. Y. Pore structure in supermacroporous polyacrylamide based cryogels. *Soft Matter* **2005**, *1*, 303−309.
(26) Hassan, A. F.; Abdel-Mohsen, A. M.; Fouda, M. M. G. Comparative study of calcium alginate, activated carbon, and their composite beads on methylene blue adsorption. *Carbohydr. Polym.* **2014**, *102*, 192−198.
(27) Lee, B. R.; Lee, K. H.; Kang, E.; Kim, D.-S.; Lee, S.-H. Microfluidic wet spinning of chitosan-alginate microfibers and encapsulation of HepG2 cells in fibers. *Biomicrofluidics* **2011**, *5*, No. 022208.
(28) Kumar, M.; Tamilarasan, R.; Sivakumar, V. Adsorption of Victoria blue by carbon/Ba/alginate beads: Kinetics, thermodynamics and isotherm studies. *Carbohydr. Polym.* **2013**, *98*, 505−513.
(29) Guo, Z.; Zhang, J.; Kang, Y.; Liu, H. Rapid and efficient removal of Pb(II) from aqueous solutions using biomass-derived activated carbon with humic acid in-situ modification. *Ecotoxicol. Environ. Saf.* **2017**, *145*, 442−448.
(30) Tan, I. A. W.; Ahmad, A. L.; Hameed, B. H. Adsorption isotherms, kinetics, thermodynamics and desorption studies of 2,4,6-trichlorophenol on oil palm empty fruit bunch-based activated carbon. *J. Hazard. Mater.* **2009**, *164*, 473−482.
(31) Masoumi, A.; Ghaemy, M. Removal of metal ions from water using nanohydrogel tragacanth gum-g-polyamidoxime: Isotherm and kinetic study. *Carbohydr. Polym.* **2014**, *108*, 206−215.
(32) Sarada, B.; Prasad, M. K.; Kumar, K. K.; Ramachandra Murthy, C. V. Cadmium removal by macro algae Caulerpa fastigiata: Characterization, kinetic, isotherm and thermodynamic studies. *J. Environ. Chem. Eng.* **2014**, *2*, 1533−1542.
(33) Kołodyńska, D.; Wnętrzak, R.; Leahy, J. J.; Hayes, M. H. B.; Kwapiński, W.; Hubicki, Z. Kinetic and adsorptive characterization of biochar in metal ions removal. *Chem. Eng. J.* **2012**, *197*, 295−305.
(34) Murcia-Salvador, A.; Pellicer, J. A.; Fortea, M. I.; Gómez-López, V. M.; Rodríguez-López, M. I.; Núñez-Delicado, E.; Gabaldón, J. A. Adsorption of Direct Blue 78 Using Chitosan and Cyclodextrins as Adsorbents. *Polymers* **2019**, *11*, No. 1003.
(35) Song, X.; Zhang, Y.; Yan, C.; Jiang, W.; Chang, C. The Langmuir monolayer adsorption model of organic matter into effective pores in activated carbon. *J. Colloid Interface Sci.* **2013**, *389*, 213−219.
(36) Jeppu, G. P.; Clement, T. P. A modified Langmuir-Freundlich isotherm model for simulating pH-dependent adsorption effects. *J. Contam. Hydrol.* **2012**, *129*−*130*, 46−53.
(37) Johnson, R. D.; Arnold, F. H. The temkin isotherm describes heterogeneous protein adsorption. *Biochim. Biophys. Acta, Protein Struct. Mol. Enzymol.* **1995**, *1247*, 293−297.
(38) Feng, N.; Guo, X.; Liang, S.; Zhu, Y.; Liu, J. Biosorption of heavy metals from aqueous solutions by chemically modified orange peel. *J. Hazard. Mater.* **2011**, *185*, 49−54.
(39) Abid, M.; Niazi, N. K.; Bibi, I.; Farooqi, A.; Ok, Y. S.; Kunhikrishnan, A.; Ali, F.; Ali, S.; Igalavithana, A. D.; Arshad, M. Arsenic(V) biosorption by charred orange peel in aqueous environments. *Int. J. Phytorem.* **2016**, *18*, 442−449.
(40) Roh, H.; Yu, M.-R.; Yakkala, K.; Koduru, J. R.; Yang, J.-K.; Chang, Y.-Y. Removal studies of Cd(II) and explosive compounds using buffalo weed biochar-alginate beads. *J. Ind. Eng. Chem.* **2015**, *26*, 226−233.
(41) Gotoh, T.; Matsushima, K.; Kikuchi, K.-I. Preparation of alginate−chitosan hybrid gel beads and adsorption of divalent metal ions. *Chemosphere* **2004**, *55*, 135−140.
(42) Cai, C.-X.; Xu, J.; Deng, N.-F.; Dong, X.-W.; Tang, H.; Liang, Y.; Fan, X.-W.; Li, Y.-Z. A novel approach of utilization of the fungal conidia biomass to remove heavy metals from the aqueous solution through immobilization. *Sci. Rep.* **2016**, *6*, No. 36546.
(43) Zouboulis, A. I.; Katsoyiannis, I. A. Arsenic Removal Using Iron Oxide Loaded Alginate Beads. *Ind. Eng. Chem. Res.* **2002**, *41*, 6149−6155.
(44) Olad, A.; Farshi Azhar, F. A study on the adsorption of chromium (VI) from aqueous solutions on the alginate-montmorillonite/polyaniline nanocomposite. *Desalin. Water Treat.* **2014**, *52*, 2548−2559.
(45) Bajpai, J.; Shrivastava, R.; Bajpai, A. K. Dynamic and equilibrium studies on adsorption of Cr(VI) ions onto binary biopolymeric beads of cross linked alginate and gelatin. *Colloids Surf., A* **2004**, *236*, 81−90.
(46) Njimou, J. R.; Măicăneanu, A.; Indolean, C.; Nanseu-Njiki, C. P.; Ngameni, E. Removal of Cd (II) from synthetic wastewater by alginate−Ayous wood sawdust (Triplochiton scleroxylon) composite material. *Environ. Technol.* **2016**, *37*, 1369−1381.

https://doi.org/10.1021/acsomega.2c03786
ACS Omega 2022, 7, 41997−42011

(47) Mondal, N. K.; Basu, S.; Sen, K.; Debnath, P. Potentiality of mosambi (*Citrus limetta*) peel dust toward removal of Cr(VI) from aqueous solution: an optimization study. *Appl. Water Sci.* **2019**, *9*, No. 116.
(48) Gopalakannan, V.; Viswanathan, N. Synthesis of magnetic alginate hybrid beads for efficient chromium (VI) removal. *Int. J. Biol. Macromol.* **2015**, *72*, 862−867.

https://doi.org/10.1021/acsomega.2c03786
ACS Omega 2022, 7, 41997−42011